Int. J. Electrochem. Sci., 14 **(2019)** 1817 – 1829, doi: 10.20964/2019.02.20

International Journal of ELECTROCHEMICAL SCIENCE
www.electrochemsci.org

PAMPS/PVA/MMT Semi-Interpenetrating Polymer Network Hydrogel Electrolyte for Solid-State Supercapacitors

Jin Wang[*], *Hucheng Chen, Yahui Xiao, Xianghu Yu, Xiaoxuan Li*

Anhui Province Key Laboratory of Advanced Functional Materials and Devices, School of Chemistry and Chemical Engineering, Hefei University of Technology, Hefei 23009, P. R. China
[*]E-mail: jinwang@hfut.edu.cn

Received: 26 September 2018/ *Accepted:* 23 November 2018 / *Published:* 5 January 2019

Polyelectrolyte hydrogels have great potential as gel-polymer electrolytes (GPE) because of their low-cost and environmental benefits. Here a polyelectrolyte hydrogel of high ionic conductivities and mechanical properties was developed via the formation of semi-interpenetrating polymer network (s-IPN) GPE, which consists of Poly (2-acrylamide-2-methyl propane sulfonic acid) (PAMPS), poly(vinyl alcohol) (PVA) and sodium montmorillonite(MMT). The additions of MMT and PVA can both increase the ionic conductivities and the tensile strength of PAMPS. PAMPS/PVA/MMT s-IPN GPE show excellent overall performance of ionic conductivity of 6.4×10^{-2} S cm^{-1} and tensile strength of 24.3 MPa when the ratio of PVA/AMPS is at 0.8:1 and MMT is at 7wt%. When PAMPS/PVA/MMT s-IPN is used as a GPE in supercapacitors, it exhibits good electrolyte behavior with its specific capacitance of 208 F g^{-1}, close to that of using 4M KOH aqueous solution electrolyte.

Keywords: hydrogel electrolyte, semi-interpenetrating, ionic conductivity, supercapacitors, Poly (2-acrylamide-2-methyl propane sulfonic acid)

1. INTRODUCTION

Liquid electrolytes are known to have high ionic conductivity but are prone to leakage and corrosion. Although solid gel electrolytes don't have these problems, but they show low ionic conductivity and poor deformability. In contrast, gel polymer electrolytes (GPE) can combine the separator and the electrolyte into a single layer, and show great advantages of compactness, reliability and freedom from leakage. In comparison to liquid and solid electrolytes, GPE show promising application in rechargeable batteries, electrochromic displays, and in particular flexible energy storage device [1-4]. Normally, GPE exhibits high conductivity between 10^{-4} and 10^{-3} S cm^{-1}[5-7]. The increasing concerns over environmental susceptibility have now stimulated the development of environmentally friend hydrogel polyelectrolytes. Although it is known the aqueous-based solid

supercapacitors has narrower voltage window [8]. The capacitance, operation voltage, energy density and power density of solid supercapacitor are all affected by the electrolytes used.

An ideal GPE for aqueous-based solid supercapacitors should possess the following properties, including high ionic conductivity at room temperature, good mechanical properties and dimensional stability, high chemical stability and sufficient film processability[9]. Various water-soluble polymers [10-13], such as poly(ethylene oxide) (PEO), poly(vinyl alcohol) (PVA), poly(acrylic acid) (PAA), poly(acrylamide) (PAAM), have been used to form GPE. PEO-based GPEs have shown high crystallinity and low ionic conductivity at the ambient temperature, whereas PAA and poly(acrylate) have higher proton conduction because of the protons in their side chains. PVA is a neutral polymer electrolyte and often used for biomedical application [14]. Aqueous PVA has excellent water retention ability which is in favor of the ion transport when used as host polymer electrolyte. To overcome the lower ionic conductivity of PVA, it has to be blended with ionic polymers or compounds with charged groups (acid, alkali or the other ionic group) [15-17]. 2-acrylamide-2-methyl propanesulfonic acid (AMPS) contains both a charged sulfonic acid groups and a hydrolysis resistant amide group that can easily form intramolecular or intermolecular hydrogen bond. Polymers made from AMPS (i.e. PAMPS and its copolymers) always possess higher conductivity compared to the neutral GPEs [18-20]. PAMPS have been blended or grafted with other polyelectrolytes to improve their performance of ion transportation, water absorption and retention capacity. The blends of PAMPS and PVA were used for methanol fuel cells membrane have been reported [21-22].

An interpenetrating polymer network (IPN) hydrogel consists of at least two intertwined polymer networks, often showing improved responsiveness and mechanical properties compared to single network hydrogels [23-25]. In the absence of across-linker, a linear polymer network can embed within the originally formed network, resulting in a semi-IPN(s-IPN). IPN hydrogels based on polyethylene glycol (PEG), PAAM and PVA are the most employed polymers of the biomedical applications. However, ionic IPN hydrogels have been only seldom reported [23]. Addition of inorganic materials, such as sodium montmorillonite (MMT), can further improve the mechanical properties, ionic conductivity and interface stability between polyelectrolyte and electrode [26].

Herein, a semi-IPN hydrogen is prepared by polymerization of AMPS monomers in a swelling PVA network with MMT as an additives. The influences of PVA and MMT on the tensile strength, ionic conductivities of PAMPS were investigated. The formation of PVA/PAMPS IPN enhances their mechanical strength and swelling response. The addition of layered MMT can increase the physical cross-link points and decrease the crystallinity of GPE, and the enhanced mechanical strength and ionic conductivity result. In comparison with our previous work of PAMPS/MMT composite hydrogel [27], the tensile strength increased from 8.3 MPa to 24.3 MPa and the ionic conductivity increased from 5.9×10^{-2} S cm^{-1} to 6.4×10^{-2} S cm^{-1}, respectively. The performance the PAMPS/PVA/MMT system used as GPE in supercapacitors was evaluated.

2. EXPERIMENTAL

2.1 Materials

AMPS (98%), PVA (98%) and N'N-methylene-bis-acrylamide (MBA) (97%) were purchased from Aladdin Co., used as received. MMT (95%) was sourced from Fenghong Co..Activated carbon (AC)with the surface area of 2000 m^2/g was from Xianfeng Nano Inc. Potassium persulfate (KPS), Potassium hydroxide (KOH) (96%), acetylene black, PVDF powder and N-methylpyrrolidone (NMP) were from Sinopharm Chemical Reagent Co. Ltd. and KPS was used after recrystallized.

2.2 Synthesis of the PAMPS/PVA/MMT s-IPN hydrogel

A series of PAMPS/PVA/MMT s-IPN electrolytes with different dosages of MMT and the weight ratios of PVA and AMPS were prepared by solution-casting method. The optimum concentrations of KPS and MBA were identified according to their influence on the ionic conductivity and tensile strength, as shown in Fig.S1 and S2 (Supporting Information). The optimized experimental procedure is as follows: 1g AMPS was dissolved in 20mL deionized water and followed by addition of MMT(7% by weight). The solution was placed in an ultrasonic bath for 0.5h to dissolve the compounds. After that, MBA crosslinker(3% byweight) was added into the solution which is placed in the ultrasonic bath for another 20 minutes. PVA(the weight ratio of PVA: PAMPS =0.8) was then dissolved in the solution using heat to generate a homogenous mixture, followed by addition of the KPS(1% in weight) water solution. The final homogenous mixture solution was poured into a PTFE mould and then in a vacuum at 60°C for 24h. The formation of PAMPS/PVA/MMT s-IPN electrolyte is illustrated in Fig.1 PAMPS/PVA s-IPN electrolyte was also prepared using the same method for comparison.

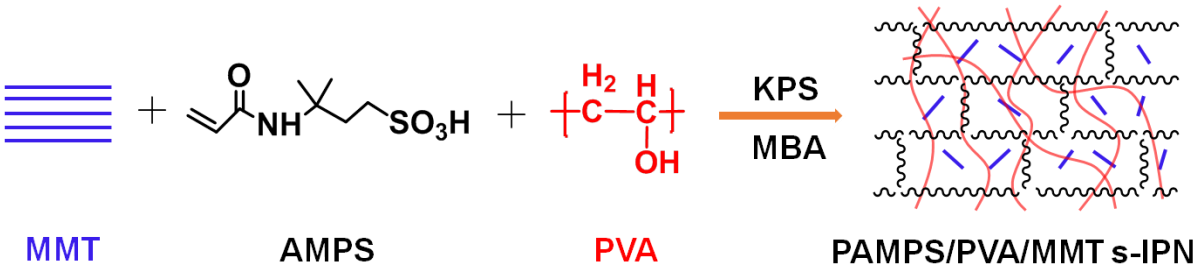

Figure 1. Schematic diagram of the formation of PAMPS/PVA/MMT-sIPN

2.3 Device Fabrication

A two-electrode supercapacitor was fabricated by sandwiching the GPE between two symmetrical AC electrodes as shown in Fig.2.The AC electrodes were prepared as reported previously [27]. Prior to use, PAMPS/PVA/MMT s-IPN hydrogel electrolytes were treated with 4mol/L KOH solution to saturate their absorption of ions.

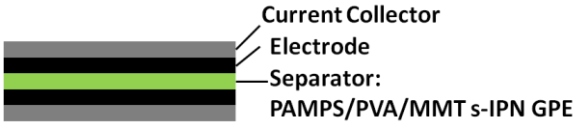

Figure 2. Schematic diagram of the capacitor model

2.4 Characterization

The structures were characterized by Fourier transform infrared spectroscopy (FT-IR) (PE 1650), X-ray diffraction (XRD) (Rigaku D/Max-2550) and scanning electron microscope (SEM) (JSM-6469LV, Japan), respectively. The thermal stability was determined by thermogravimetric analysis (TGA) (Netzsch TG 209 F3). Mechanical properties were tested by a CMT4104 electronic universal tester (MTS Ind. Co.,) with 10 mm/min stretched velocity.

The electrochemical performance was conducted using a CHI660B electrochemical workstation. The ionic conductivity is measured by electrochemical impedance spectroscopy (EIS) in the frequency range between 0.01 Hz and 100 kHz with a perturbation of 5 mV rms. The GPE was sandwiched by two stainless steels with the mode of SS/ PAMPS/PVA/MMT s-IPN /SS (SS notes stainless steels). The bulk ionic conductivity (σ) of the polyelectrolyte was calculated according to the equation in literature [28]. The cyclic voltammograms (CV) and galvanostatic charge-discharge measurements (GCD) were tested by a two-electrode method, and the specific capacitance (C) of the supercapacitor was calculated according to the equation in literature [29].

3. RESULTS AND DISCUSSION

3.1 Structural Characterization

As shown in Fig.3, the characteristic absorption peaks of PAMPS(1646 cm^{-1}, 1559cm^{-1} of NH bonds, 1372$cm^{-1}$of S=O of PAMPS) and MMT(1036 cm^{-1}, 461 cm^{-1} of Si-O band, 522 cm^{-1} of Si-O-Al) were observed in the infrared spectra of PAMPS/PVA and PAMPS/PVA/MMT s-IPN, indicating the existence of PAMPS and MMT clay layers. In the FT-IR spectrum of PVA, the absorption peak of C-O stretching is at 1098 cm^{-1}. However, in the FT-IR spectra of PAMPS/PVA s-IPN and PAMPS/PVA /MMT s-IPN, the absorption peak of C-O stretching moves to 1040 cm^{-1}, which can be attributed to the formation of hydrogen bonds between the -OH of PVA and amide group of PAMPS [30]. Thus the s-IPN structures were formed in both PAMPS/PVA and PAMPS/PVA/MMT.

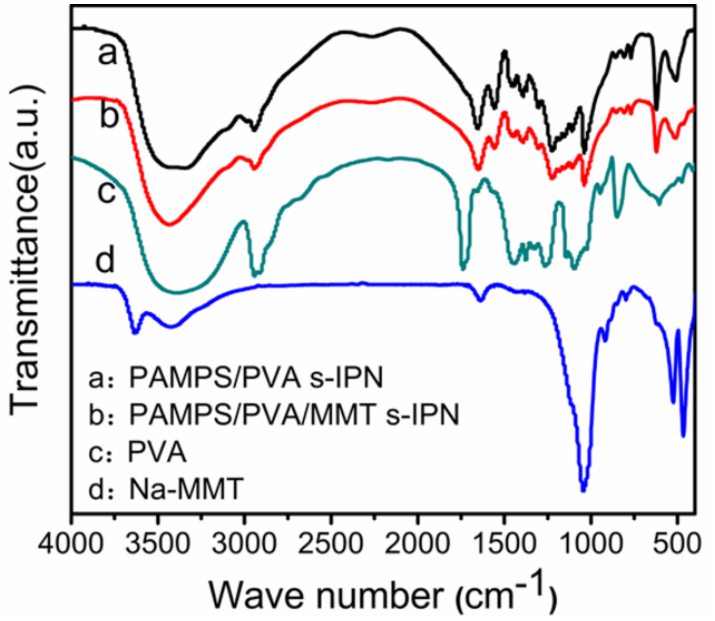

Figure 3. FTIR spectra of (a) PAMPS/PVA s-IPN, (b) PAMPS/PVA/MMT s-IPN,(c) PVA and (d) MMT

The crystallization of polymer and the laminar structure of clay were illustrated by their XRD patterns, shown in Fig. 4. The Na-MMT crystals show diffraction peaks at 7.0°, 19.8°, 26.6°, 28.4°, 27.9°, 34.9° and 42.3°. However, the (001) lattice face of MMT at 2θ = 7.0° disappeared in the XRD Patten of the PAMPS/PVA/MMT s-IPN, indicating the MMT layer has been exfoliated in the s-IPN hydrogel and consequently a collapsed crystal structure.

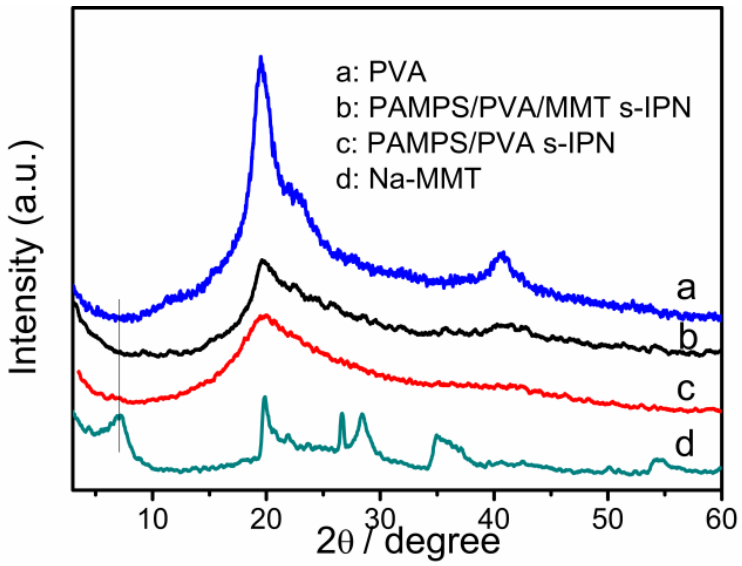

Figure 4. XRD patterns of (a) PVA, (b)PAMPS/PVA/MMT s-IPN, (c) PAMPS/PVA s-IPN and (d) MMT

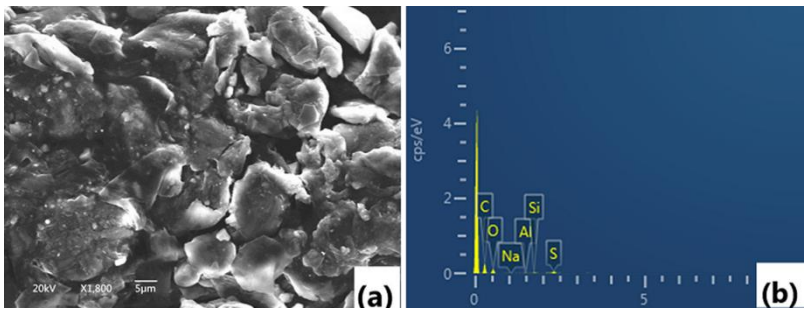

Figure 5. SEM(a) and EDX(b) image of PAMPS/PVA/MMT s-IPN GPE

The pure PVA system show the diffraction peaks at 19.5° and 40.7°. In contrast, the characteristic peak at 40.7° is hardly observable and the peak at 19.5° is significantly reduced in the XRD patterns of PAMPS/PVA s-IPN and PAMPS/PVA/MMT s-IPN. These changes are likely due to the amorphous domain of PVA polymer matrix in the s-IPN network, which restrict the regular stack of molecular chains into acrystalline domain. The SEM images of PAMPS/PVA/MMT s-IPN (Fig.5(a)) further illustrated a loose, coarse structure of the hydrogel consisting of a large number of micropores. The EDX spectra of PAMPS/PVA/MMT s-IPN (Fig.5(b)) reveals the presence of C, O, S, Si, Na and Al elements, which is consistent with the charge ratio of MMT in the PAMPS/PVA/MMT s-IPN system.

3.2 Mechanical Properties Test

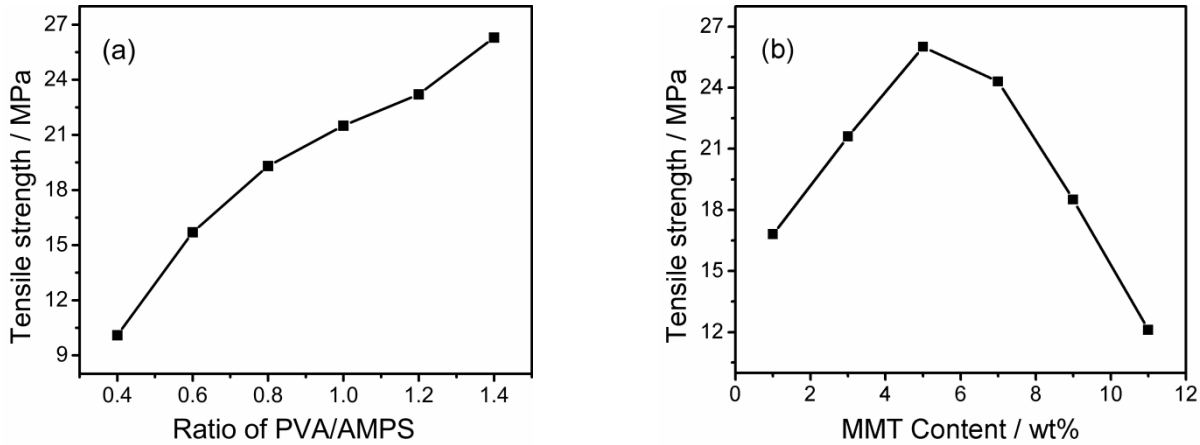

Figure 6. (a) The tensile strength of PAMPS/PVA s-IPN with different ratio of PVA to AMPS, (b) The tensile strength of PAMPS/PVA/MMT s-IPN with different amounts of MMT at 0.8 (ratio of PVA/PAMPS)

The addition of PVA and MMT can influence the tensile strength of PAMPS/PVA/MMT s-IPN hydrogels. As shown in Fig.6(a), the tensile strength of PAMPS/PVA s-IPN increased with the increase in the ratio of PVA to AMPS. This is partially due to the stronger mechanical property of PVA, and partially due to the formation of hydrogen bonds between PVA and PAMPS in the s-IPN. At the fixed ratio of PVA/PAMPS at 0.8, the increase of MMT leads to an initial increase in the tensile strength of

the s-IPN followed by a rapid decrease after it reaches the maximum strength of 24.3MPa (Fig.6(b)).This shows that the well-dispersed inorganic particles in polymer can act as physical cross-linking points to increase the mechanical properties. However, overloading of MMT can also lead to poor dispersed MMT in the network and resulting the phase separation between the organic and inorganic phases.

Fig.7 is the tensile strength comparison diagram of PAMPS/MMT, PAMPS/PVA s-IPN and PAMPS/PVA/MMT s-IPN hydrogels. The influence of MMT and s-IPN structure on the tensile strength of the hydrogels can be showed visually. The addition of PVA to the s-IPN can significantly increase the tensile strength, and a further addition of suitable amount of MMT can further improve the mechanical strength of the s-IPN.

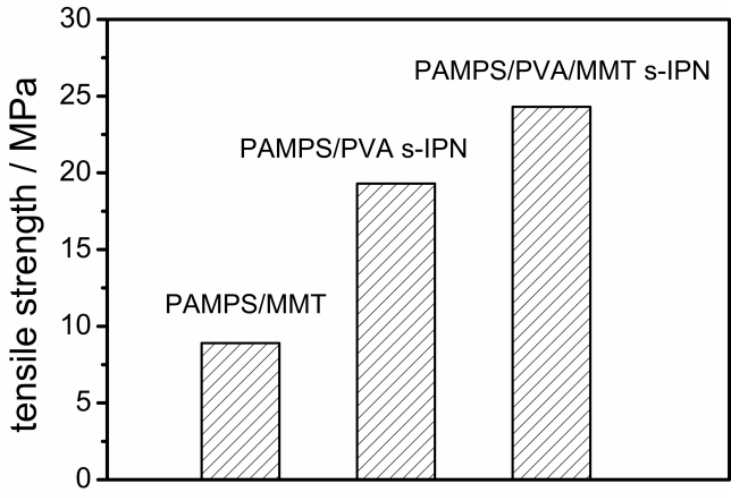

Figure 7. The tensile strength comparison diagram

3.3 Thermal Properties Analysis

The thermal behavior of PAMPS/PVA and PAMPS/PVA/MMT s-IPN hydrogel was shown in the TGA curves in Fig.8. The weight loss around 180℃ was observed in both s-IPNs, which can be attributed to the decomposition of the residual water, bound water, amino groups and the other side groups of PAMPS and PVA. Compared to PAMPS/PVA s-IPN, PAMPS/PVA/MMT s-IPN has a plateau region from 180℃ to 250℃, indicating better thermostability. It is not surprising considering the interactions between inorganic ions in layers of MMT and the sulphonic groups of PAMPS. The decomposition above 250℃ was observed in both case and is due to the degradation of the sulphonic groups. The final major decomposition step between 300℃ and 500℃ may be due to the cleavage of the backbone of PVA. The thermal properties are consistent with that of the PVA/PAMPS/ZIF ternary composite [21], suggesting the improvement effect of inorganic material on the thermostability.

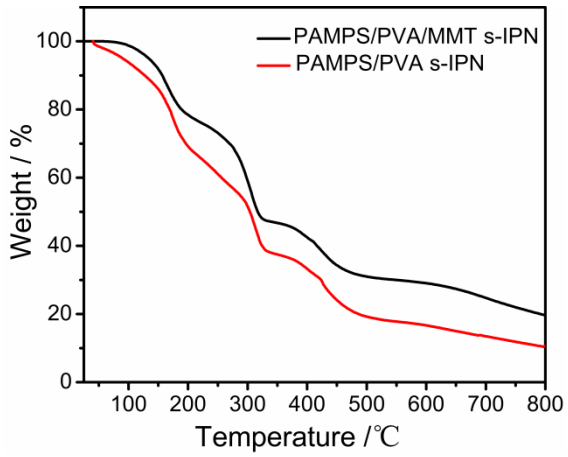

Figure 8. TG curves of PAMPS/PVA and PAMPS/PVA/MMT s-IPN GPE

3.4 Ionic Conductivity Studies

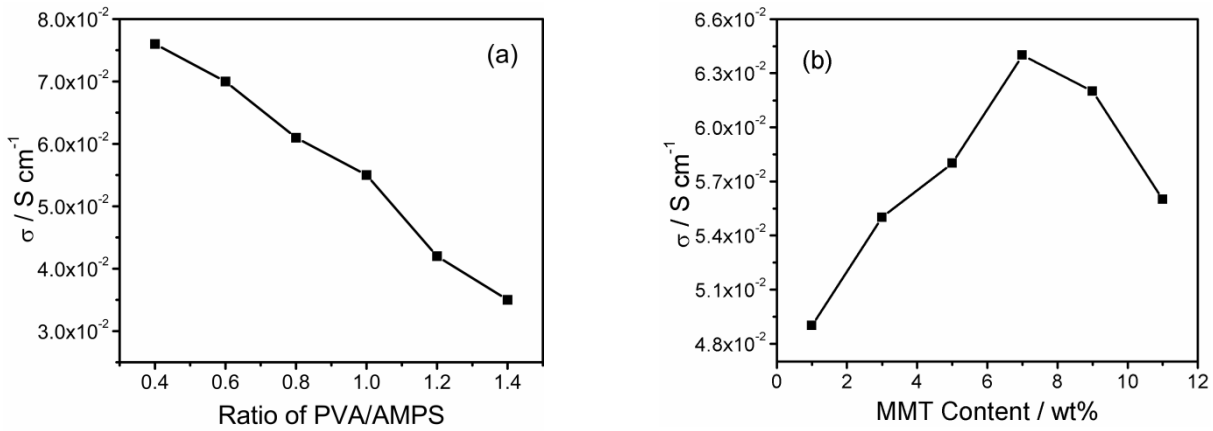

Figure 9. (a) Ionic conductivities of PAMPS/PVA s-IPN with different ratio of PVA to AMPS, (b) Ionic conductivities of PAMPS/PVA/MMT s-IPN with different amounts of MMT at 0.8 (ratio of PVA/PAMPS)

The influence of the addition of PVA and Na -MMT on the ionic conductivity of s-IPNs was shown in Fig.9. The ionic conductivity of the PAMPS/PVA s-IPN hydrogel decreased with increasing the ratio of PVA/AMPS(Fig.9(a)), suggesting the ionic conductivity of the s-IPN mainly comes from the anionic structure of AMPS monomer. The amide group of PAMPS can increase the ionic concentration of the hydrogels. The influence of MMT on the ionic conductivity (Fig.9(b)) is similar to that on the tensile strength (Figure 6b), where initial increase was observed with the increase of MMT amount and followed by the sharp decrease (i.e. the ratio of PVA/PAMPS is fixed at 0.8). The maximum ionic conductivity of PAMPS/PVA/MMT s-IPN hydrogel is 6.4×10^{-2} S cm^{-1} at room temperature (Fig. 9b). In comparison with the 1.2×10^{-2} S cm^{-1} at 100 °C of PVA/PAMPS blends (the mass ratio of PVA/PAMPS is 1:3)[22], PAMPS/PVA/MMT s-IPN GPE shows the better ionic transport performance. PVA/PAMPS/ZIF ternary composite has the conductivity of 0.134 S cm^{-1} at 80 °C (the mass ratio of

PVA:PAMPS:ZIF-8 is 55:40:5)[21], which is due to the increasing temperature improved the rate of electrolyte dissociation and thus the ionic conductivity increased. Although the ion-exchange capability of can facilitate the transportation of ion entrapped in PAMPS/PVA/MMT s-IPN hydrogel, overloaded MMT can result in the phase separation.

Fig.10 is the ionic conductivity comparison diagram of PAMPS/MMT, PAMPS/PVA s-IPN and PAMPS/PVA/MMT s-IPN hydrogels. The influence of MMT and s-IPN structure on the ionic conductivity of the hydrogels can be showed visually. The addition of MMT has clear enhancement on the ionic conductivity of a s-IPN. This improvement partially comes from the increased tensile strength caused by the addition of MMT particles, which perhaps improve the stability between polyelectrolyte and electrode interface. The presentation of MMT could also reduce the crystalline phase and thus benefit ion transport within the polyelectrolyte. In addition, MMT shave good ion-exchange capability and can directly contribute to ionic conductivity. It should be noted the ionic conductivity of PAMPS/PVA/MMT s-IPN is higher than that of PAMPS/MMT (Fig. 10), suggesting a beneficial influence on conductive ability from a hydrophilic polymer, such as PVA.

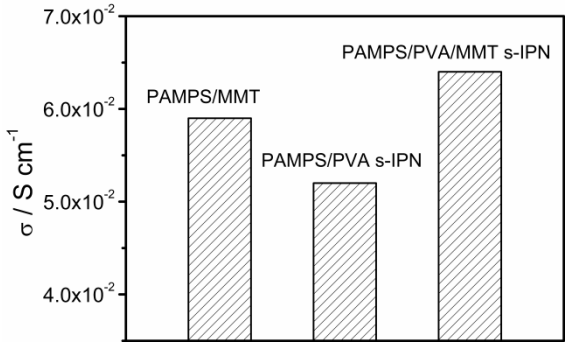

Figure 10. The ionic conductivity comparison diagram

3.5 Electrochemical Performance Studies

Electrochemical performance of the PAMPS/ PVA/MMT s-IPN GPE was determined in a potential range of 0 ~ 1.8 V at the scan rate of 20 mV/s. Fig.11(a) show the rectangular shapes of the two CV plots, indicating a small equivalent series resistance [31]. Capacitors using PAMPS/PVA/MMT s-IPN GPE has higher specific capacitance value than that of PAMPS/PVA s-IPN GPE. The CV plots of supercapacitor assembled with PAMPS/PVA/MMT s-IPN GPE at different scan rates are showed in Fig.11(b). The increase of the scan rate increases the current but the CV plots maintain the same shape. This behavior is in accordance with the equation $I = CdV / dt$ of an electronic double layer capacitor. The currents are quite stable during the electrochemical cycling, suggesting smooth ion transport in the polymer matrix.

GCD curves for the supercapacitors with the PAMPS/PVA/MMT s-IPN GPE, PAMPS/PVA s-IPN GPE and 4M KOH aqueous solution at a current density of 10mA g-1are shown in Fig.11(c). All three electrolytes show similar linear and symmetric trends, implying good ion transportation and interfacial contact between s-IPN GPE and the electrode. The specific capacitances of supercapacitor

based on 4M KOH aqueous solution electrolytes, PAMPS/PVA/MMT s-IPN GPE and PAMPS/PVA s-IPN GPE are 208 F g^{-1}, 201 F g^{-1} and 171 F g^{-1}, respectively. In comparison with our previous work of PAMPS/MMT composite hydrogel [27], the great extent improvement of specific capacitances should attribute to the using of AC electrode with higher specific surface area. The capacitance of PAMPS/PVA/MMT s-IPN GPE was closed to that of 4 M KOH aqueous solution electrolyte, suggesting its good ion transport capability. Comparing with PAMPS/PVA s-IPN GPE, the higher capacitance of PAMPS/PVA/MMT s-IPN GPE may due to the doping of ionic MMT in PAMPS/PVA s-IPN. The charge-discharge cycles at a current density of 50 mA g^{-1} were tested for evaluating the stability of supercapator. As shown in Fig.11(d), the PAMPS/PVA/MMT s-IPN GPE based supercapator shows a better stability and has a 91% retention up to 1000 cycles in comparison with 72% retention of PAMPS/PVA s-IPN GPE.

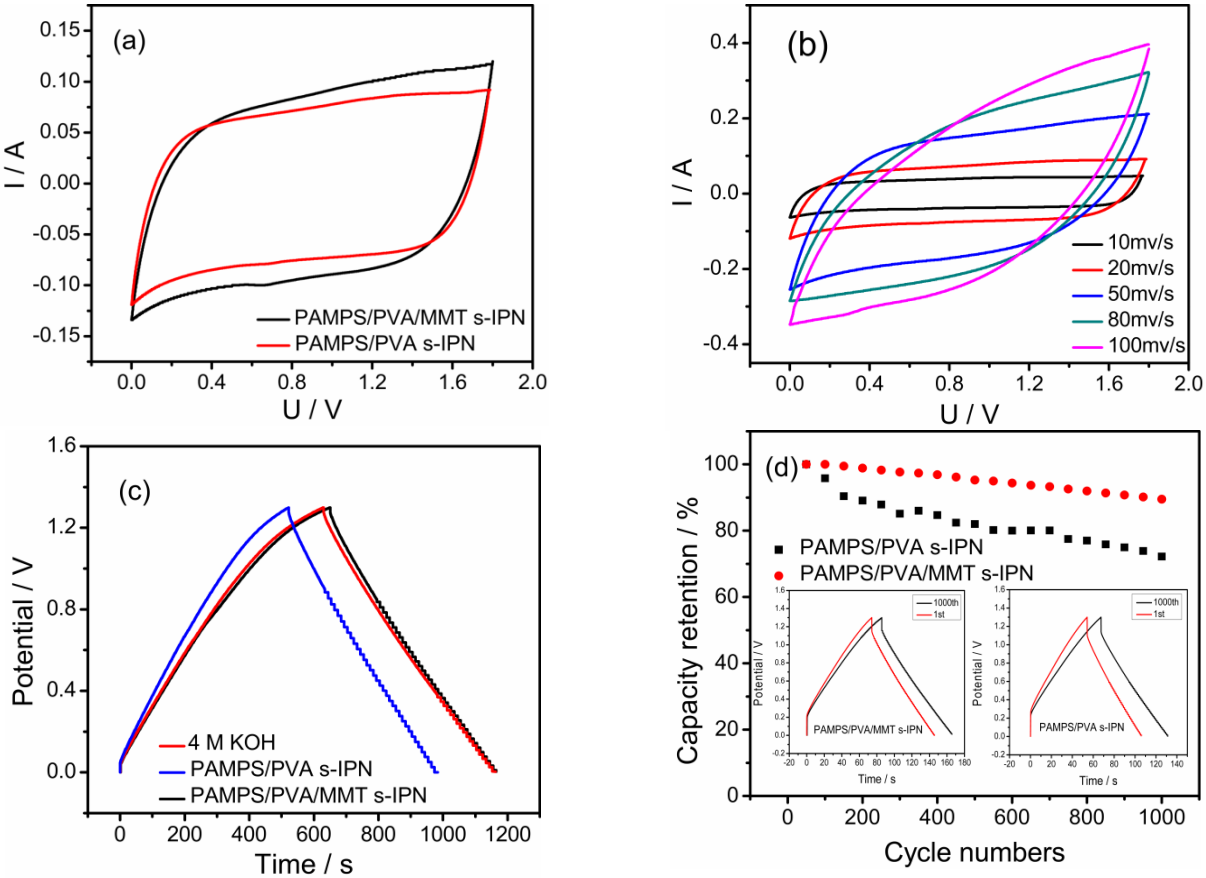

Figure 11. Electrochemical properties of capacitors based on PAMPS/PVA and PAMPS/PVA/MMT s-IPN GPE (a) CV plots, (b) CV plots at different scan rates, (c) GCD curves with PAMPS/PVA/MMT s-IPN GPE, PAMPS/PVA s-IPN GPE and 4 M KOH aqueous solution electrolyte, (d) Cycling stability

4. CONCLUSION

PAMPS/PVA/MMT s-IPN hydrogels with high ionic conductivities and tensile strength were developed with MBA as a cross-linker and KPS as an initiator. Both MMT and PVA can improve the ionic conductivities and tensile strength of the s-IPN hydrogel. The -OH groups of PVA form hydrogen bonds with the amide groups of PAMPS, thus forming the s-IPN structure and enhancing the mechanical strength. The addition of layered MMT can also increase the physical cross-link points and decrease the crystallinity of GPE, and then enhanced the mechanical strength and ionic conductivity of the hydrogel. With KOH solution as the conducting salt, capacitors using PAMPS/PVA and PAMPS/PVA/MMT s-IPN electrolytes show typical characteristics for an electronic double-layer capacitance. Capacitor consisting of PAMPS/PVA/MMT s-IPN shows good cycling stability with its specific capacitance closes to that of using liquid electrolyte (4M KOH aqueous solution electrolyte), suggesting the promising potential for the PAMPS/PVA/MMT s-IPN GPE in the field of solid supercapacitor.

SUPPORTING MATERIAL:

KPS is the initiator used for the polymerization in the system. Ionic conductivity and tensile strength of PAMPS/PVA s-IPN hydrogel as a function of KPS loading is shown in Figure S1. The ionic conductivities and tensile strength of PAMPS/PVA s-IPN hydrogel initially increase with the amount of KPS and then decrease with additional loading – the same behavior as the addition of MMT. The optimum KPS dosage is 1.0wt%. The low concentration of KPS led to the PAMPS of high molecular weight and thus high degree of swelling. This favors entrapping conducting liquid (4 M KOH), resulting in high ionic conductivity. Higher loading of KPS increase the concentration of free radical sand consequently the PAMPS of lower molecular weight. This corresponds to a lower swelling capacity, decreased ionic conductivity and weaker tensile strength.

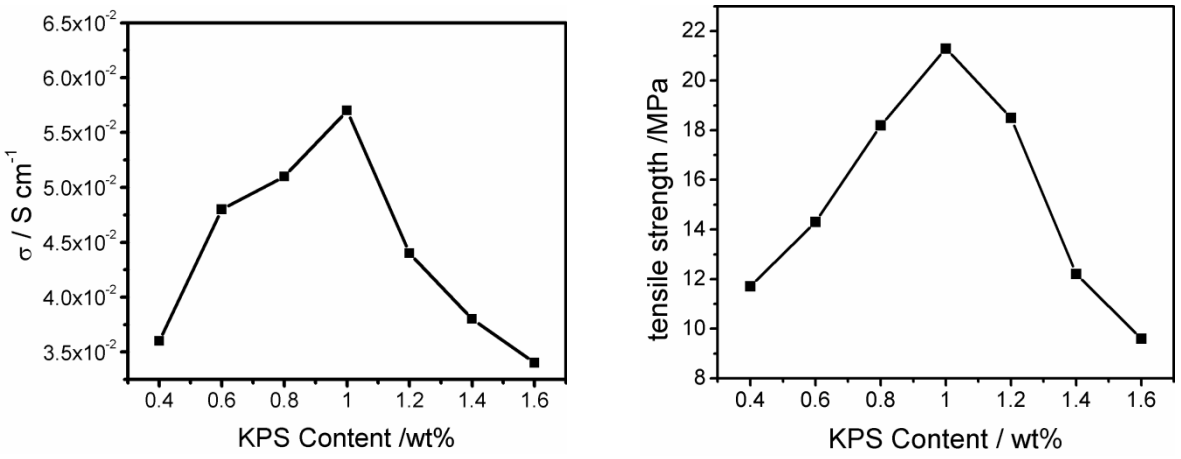

Figure S1. Ionic conductivity and tensile strength of PAMPS/PVA s-IPN hydrogel as a function of KPS loading weights

Ionic conductivity and tensile strength of PAMPS/PVA s-IPN hydrogel as a function of MBA loading is shown in FigureS2.The ionic conductivity of PAMPS/PVA s-IPN hydrogel decreased with the increasing of MBA as a result of the increased cross-linking density. The tensile strength of PAMPS/PVA s-IPN hydrogel increased first and then decreased with the increase of MBA. The tensile strength is 21.7 MPa when the content of MBA is 4wt%.With the excess amount of MBA, the reaction between MBA and PAMPS occurs. This not only inhibits the extension of PAMPS polymer chain but also the interpenetrating structure between PAMPS and PVA.

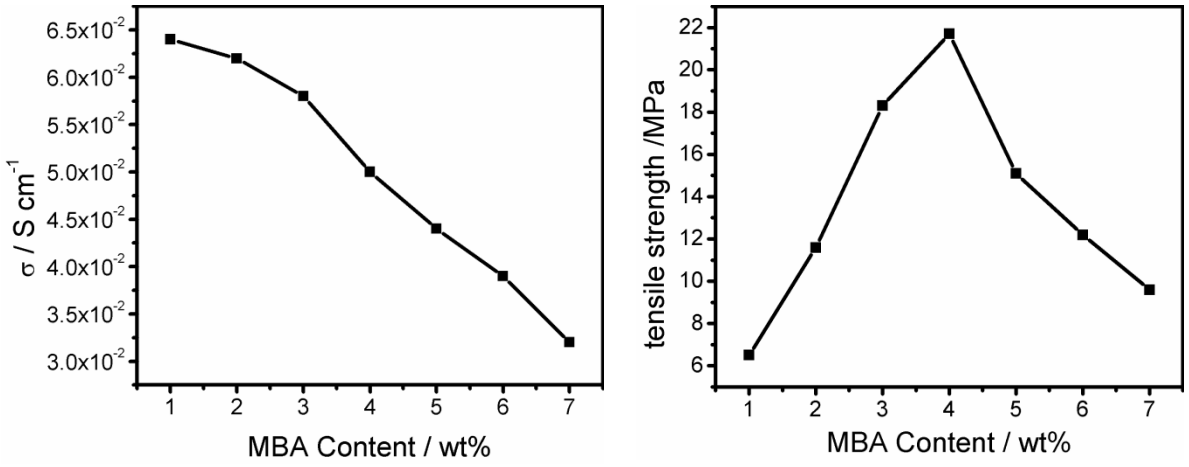

Figure S2. Ionic conductivity and tensile strength of PAMPS/PVA s-IPN hydrogel as a function of MBA loading weights

References

1. A.M. Stephan, *Eur. Polym. J.*, 42(2006) 21-42.
2. S.S. He, L.B. Qiu, L. Wang, J.Y. Cao, S.L. Xie, Q. Gao, Z.T. Zhang, J. Zhang, B.J. Wang, H.S. Peng, *J. Mater. Chem. A*, 4(2016)14968-14973.
3. M.M. Eldin, A.E. Hashem, T.M. Tamer, A.M. Omer, M.E. Yossuf, M.M. Sabet, *Int. J. Electrochem. Sci.*, 12(2017) 3840-3858.
4. J. Bae, M.K. Song, Y.J. Park, J.M. Kim, M. Liu, Z.L. Wang, *Angew. Chem. Int. Ed.*, 50(2011) 1683-1687.
5. M.K. Singh, M. Suleman, Y. Kumar, S.A. Hashmi, *Energy*, 80(2015)465-473.
6. A.A. Łatoszyńska, G.Z. Żukowska, I.A. Rutkowska, P.L. Taberna, P. Simon, P. J. Kulesza, W. Wieczorek, *J. Power Sources*, 274(2015)1147-1154.
7. L. Yang, J. Hu, G. Lei, H. Liu, *Chem. Eng. J.*, 258(2014)320-326.
8. A. Ponrouch, D. Monti, A. Boschin, B. Steen, P. Johansson, M.R. Palacin, *J. Mater. Chem. A.*, 3(2015)22-42.
9. H. Gao, K. Lian, *RSC Adv.*, 4(2014) 33091-33113.
10. S. Ketabi, K. Lian, *Solid State Ionics*, 227(2012)86-90.
11. F.D. Yu, M.L. Huang, J.H. Wu, Z.Y. Qiu, L.Q. Fan, J.M. Lin, Y.B. Lin, *J. Appl. Polym. Sci,.* 131(2014) 39784.
12. K.M. Kim, J.H. Nam, Y.G.Lee, W.I. Cho, J.M. Ko, *Curr. Appl. Phys.*, 13(2013)1702-1706.
13. I. Stepniak, A. Ciszewski, *ElectrochimActa*, 56(2011) 2477-2482.

14. A.S. Hoffman, *Adv. Drug Deliv. Rev.*, 64(2012)18-23.
15. M.H. Hussin, N.A. Husin, I. Bello, N. Othman, M. Abu Bakar, M.K.M. Haafiz, *Int. J. Electrochem. Sci.*, 13(2018)3356-3371.
16. S.B. Lin, C. H. Yuan, A.R. Ke, Z.L. Quan, *Sensors Actuat. B: Chem.,* 134 (2008) 281-286.
17. G. Wee, O. Larsson, M. Srinivasan, M. Berggren, X. Crispin, S. Mhaisalkar, *Adv. Funct. Mater.,* 20 (2010) 4344-4350.
18. Chikh, S.Girard, D. Teyssie, O. Fichet, *J. Appl. Polym. Sci.*, 107(2008) 3672-3680.
19. L. Ahmadian-Alam, M. Kheirmand, H. Mahdavi, *Chem. Eng. J.*, 284(2016) 1035-1048.
20. R. Shahabadi, M. Abdollahi, A. Sharif, *Int. J. Hydrogen Energy*, 40(2015)3749-3761.
21. M. Erkartal, H. Usta, M. Citir, U. Sen, *J. Membr. Sci.*, 499(2016)156-163.
22. C. A. Dai, C.J. Chang, A. C. Kao, W.B. Tsai, W. S. Chen, W. M. Liu, W. P. Shih, C.C. Ma, *Sensors Actuat. A: Phys.*, 155(2009)152-162.
23. E.S. Dragan, *Chem. Eng. J.*,243(2014) 572-590.
24. L. Chikh, V. Delhorbe, O. Fichet, *J Membrane Sci.*, 368(2011) 1-17.
25. J. Hu, T. Kurokawa, K. Hiwatashi, T. Nakajima, Z.L. Wu, S. M. Liang, J.P. Gong, *Macromolecules,* 45(2012) 5218-5228.
26. A. Karimi, W. M. A. Wan Daud, *Polym. Compos.*, 37(2016) 897-906.
27. J. Wang, X.H. Yu, C. Wang, K.C. Xiang, M.D. Deng, H.B. Yin, *J. Alloys. Compds.*, 709(2017)596-601.
28. N.A. Choudhury, A.K. Shukla, S. Sampath, S. Pitchumani, *J. Electrochem. Soc.*, 153(2006)A614-A620.
29. G.P. Pandey, S.A. Hashmi, *ElectrochimActa*, 105(2013)333-341.
30. S.B. Lin, C.H. Yuan, A.R. Ke, Z.L. Quan, *Sensors Actuat. B: Chem.*, 134(2008)281-286.
31. Q. Guo, X. Zhou, X. Li, S. Chen, A. Seema, A. Greiner, H. Hou, *J. Mater. Chem.*, 19(2009)2810-2816.